Progress In Electromagnetics Research Letters, Vol. 62, 9–15, 2016

Polarization Conversion Metasurface for Broadband Radar Cross Section Reduction

Wen Jiang, Yu Xue*, and Shu-Xi Gong

Abstract—A novel polarization conversion metasurface (PCM) is proposed and applied to radar cross section (RCS) reduction. The proposed design has the advantage of simple geometry while simultaneously reducing RCS over broadband. The metasurface is created by the combination of an oblique split ring resonator (SRR) and a cut-wire resonator, which is capable of converting a linear polarization state into its orthogonal one. The simulation results show that the 10 dB bandwidth of polarization conversion is obtained in wideband from 9.4 to 19.2 GHz, with an average polarization conversion ratio (PCR) of nearly 100%. Due to the high PCR, RCS reduction of 10 dB can be realized over 60% frequency bandwidth with respect to the equal-sized PEC ground plane. The maximum reduction is 32.8 dB. To validate the simulation results, prototypes of the PCM are fabricated and measured. Excellent agreement between simulations and measurements is achieved.

1. INTRODUCTION

A lot of attention has been focused on radar cross section (RCS) reduction with the rapid development of stealth technology. Metasurface, as an alternative means, has played an important role in terms of low RCS with a low profile configuration.

Two common methods have been proposed in literature for RCS reduction. One is changing the shape of the object [1] and the other is loading radar absorbing materials (RAM) or coatings [2]. The former one redirects the scattered energy away from the source while the latter one transforms the radio frequency energy into heat. In addition, there are also other techniques for RCS reduction, such as employing frequency selective surface (FSS) radome [3], as well as loading electromagnetic band-gap (EBG) radio absorbers [4]. Nevertheless, a shared drawback to these methods is narrow bandwidth.

In last few years, there are plenty of applications for RCS reduction by utilizing chessboard configuration based on the passive phase cancelation [5–9]. In the beginning, Paquay et al. proposed a planar structure consisting of a combination of artificial magnetic conductors (AMC) and perfect electric conductors (PEC) in a chessboard configuration, which has shown the ability of redirecting the backscattering energy away from the boresight direction [5]. However, the bandwidth of RCS reduction is restricted by the in-phase reflection of AMC. To expand the bandwidth, many researches have been done [6–9]. As an example, a wider RCS reduction band is achieved by means of combining AMCs of different sizes [6, 7]. In [8] and [9], a method that uses two different types of AMCs was presented.

Recently, designs for RCS reduction based on the principle of polarization conversion have been reported [10–12]. For instance, Liu et al. proposed and experimentally verified a polarization conversion metasurface (PCM) composed of fishbone-shaped arrays which can generate several separate narrow bands [10]. To overcome the bandwidth limitation, a novel type of PCM is proposed and analyzed in this paper. Based on the polarization conversion strategy, we succeed to replace two different types of

Received 5 June 2016, Accepted 26 August 2016, Scheduled 29 August 2016

* Corresponding author: Yu Xue (xy18392051519@163.com).

The authors are with the National Key Laboratory of Antennas and Microwave Technology, Xidian University, Xi'an, Shaanxi 710071, China.

AMCs [8, 9] with one structure. The metasurface is created by the combination of an oblique SRR and a cut-wire resonator. Owing to the high PCR, a wide 10 dB monostatic RCS reduction bandwidth from 10.2 to 19.3 GHz is achieved.

This paper is organized as follows. In Section 2, the design and principle of the PCM are introduced, which is followed by the fabrication and measurements of the PCM in Section 3. Finally, conclusions are drawn in Section 4.

2. DESIGN OF THE PROPOSED PCM

2.1. Design of the PCM Unit Cell

In [13] and [14], a cut-wire resonator and a double V-shaped resonator are proposed to realize linear polarization conversion, respectively. Inspired by the researches, a novel type of PCM for RCS reduction is designed in this paper. The unit cell geometry of the proposed PCM and metallic ground sheet separated by a substrate are depicted in Fig. 1(b). The dielectric layer is selected as F4B-2, with a relative permittivity of 2.65, loss tangent of 0.001, and thickness $h = 3$ mm. The metallic layer is modeled as a copper film with a thickness of 0.018 mm and electrical conductivity $\sigma = 5.8 \times 10^7$ S/m. To obtain wide polarization conversion bandwidth, final optimization has been performed. The optimal geometrical dimensions are exhibited in Fig. 1(a), in which $l = 3.05$ mm, $p = 1.3$ mm, $w = 0.15$ mm, $r_1 = 2.15$ mm, $r_2 = 1.95$ mm, $r_3 = 1.4$ mm and $r_4 = 1.2$ mm. The periodicity of the unit cell structure is $a = 5$ mm. In the following, we adopt the definitions of co- and cross-polarization reflection coefficients and the polarization conversion ratio (PCR) put forward from [14], where the co- and cross-polarization reflection coefficients can be defined as $r_{xx} = |\vec{E}_{xr}|/|\vec{E}_{xi}|$ and $r_{yx} = |\vec{E}_{yr}|/|\vec{E}_{xi}|$ for x-polarized incidence. Here, $\vec{E}_{xi}$ denotes the electric field of the x-polarized incident EM wave; $\vec{E}_{xr}$ and $\vec{E}_{yr}$ indicate the electric

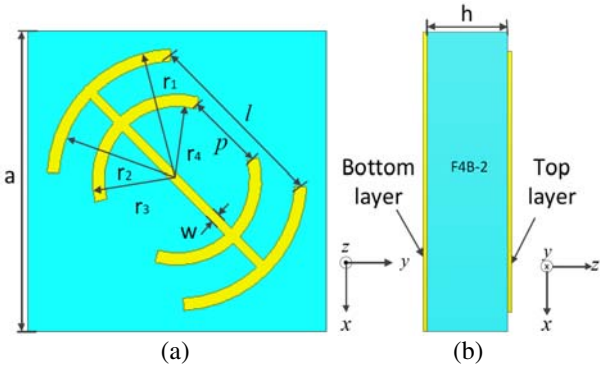

Figure 1. Geometry of the PCM unit cell, (a) top view and (b) side view.

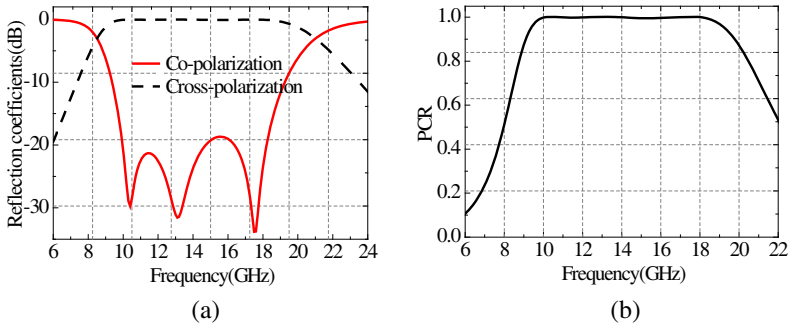

Figure 2. Simulated reflections of the periodic unit cell. (a) The co- and cross-polarization reflection coefficients and (b) the polarization conversion ratio (PCR).

field of the x- and y-polarized reflected EM waves, respectively. Then, the polarization conversion ratio (PCR) can be expressed as $PCR = r_{yx}^2/(r_{xx}^2 + r_{yx}^2)$ for x-to-y polarization conversion. Reflection characteristics of the unit cell are carried out by full-wave electromagnetic (EM) simulation software Ansoft HFSS 15.

To verify the effect of the PCM on polarization conversion, the co- and cross-polarization reflection coefficients and PCR of the periodic unit cell under a normally incident wave are illustrated in Fig. 2. As shown in Fig. 2(a), the 10 dB bandwidth of polarization conversion is from 9.4 to 19.2 GHz. Within the 10 dB bandwidth, the average PCR reaches almost 100%.

2.2. Mechanism of Wideband Polarization Conversion

To investigate the principle of polarization conversion on the PCM unit cell, a schematic diagram is presented in Fig. 3. The unit cell structure can be regarded as a combination of an oblique SRR and a cut-wire resonator, which can support "symmetric" and "antisymmetric" modes excited by components of the incident field along v- and u-axes, respectively [15].

Take a normally x-polarized incident wave as an example. The incident wave $\vec{E}_i$ can be decomposed into two perpendicular components along u- and v-axes, respectively. Then, the incident EM wave can be expressed as $\vec{E}_i = \vec{u}\vec{E}_{iu} + \vec{v}\vec{E}_{iv}$, and the reflected wave as $\vec{E}_r = \vec{u}\vec{E}_{ru} + \vec{v}\vec{E}_{rv}$. In the symmetric mode, the proposed structure behaves as a PEC because of the electric resonance, leading to the opposite phase between $\vec{E}_{iv}$ and $\vec{E}_{rv}$. In the antisymmetric mode, the function can be considered as high impedance surface because of the magnetic resonance, which makes $\vec{E}_{iu}$ in-phase with $\vec{E}_{ru}$. Hence, the synthetic fields for$\vec{E}_{ru}$ and $\vec{E}_{rv}$ will be along the y-axes, as demonstrated in Fig. 3(a). Likewise, the polarization conversion can be realized by the mirror unit cell in Fig. 3(b).

To figure out the mechanism of wideband polarization conversion with the proposed structure, the surface current distributions on the PCM unit cell and metallic ground sheet are studied at three resonant frequencies of 10.4, 13.1 and 17.5 GHz, respectively, as revealed by Figs. 4(a)–(c). In the v-polarized case, the currents on the PCM unit cell flow from the cut-wire resonator to the double SRR, which can be viewed as an electric dipole. Differently, in the u-polarized case, the currents on the PCM unit cell flow mainly along the double SRR, which makes the unit cell equivalent to a cut-wire resonator. Moreover, the induced currents on the ground sheet arise from the surface currents on the PCM unit cell. We can judge the resonance type through the directions between the surface currents on the PCM unit cell and the ground sheet. As shown in Figs. 4(a) and (b), the surface currents on the PCM unit cell are antiparallel to those induced on the ground sheet, which produce the magnetic resonances. On the contrary, the surface currents on the PCM unit cell are parallel to those induced on the ground sheet in Fig. 4(c), which generate the electric resonance. The multiple resonance characteristic contributes to the wide polarization conversion bandwidth.

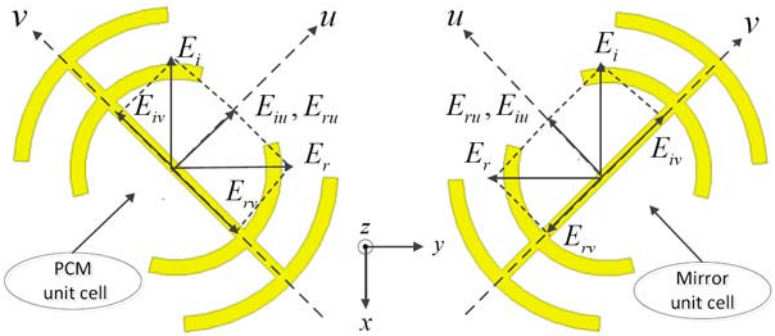

(a) (b)

Figure 3. Intuitive scheme of x-to-y polarization conversion for (a) the PCM unit cell and (b) the mirror unit cell.

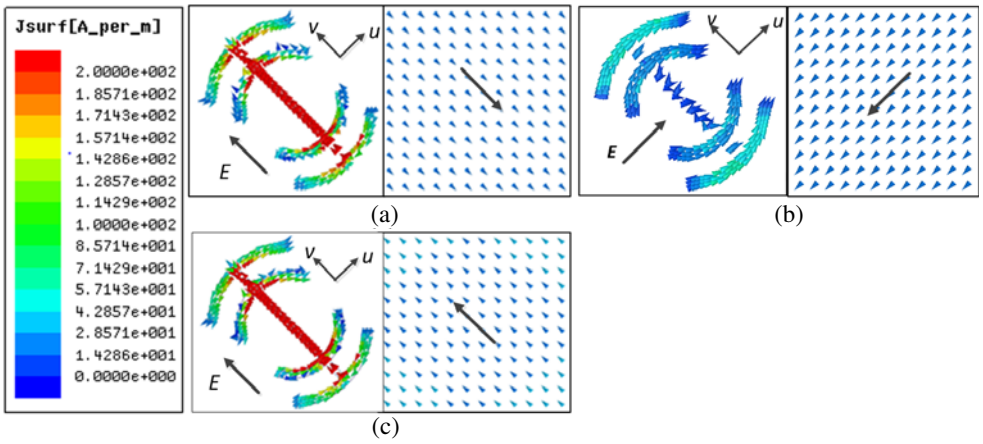

Figure 4. Surface current distributions on the metasurface unit cell and metallic ground sheet at Three resonant frequencies. (a) 10.4 GHz, (b) 13.1 GHz, and (c) 17.5 GHz.

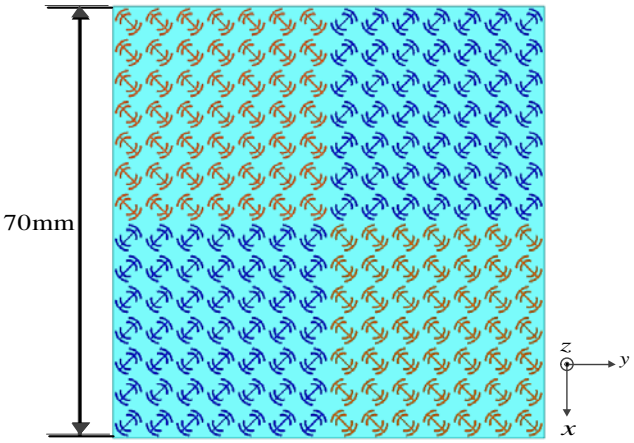

Figure 5. The geometry of the proposed PCM.

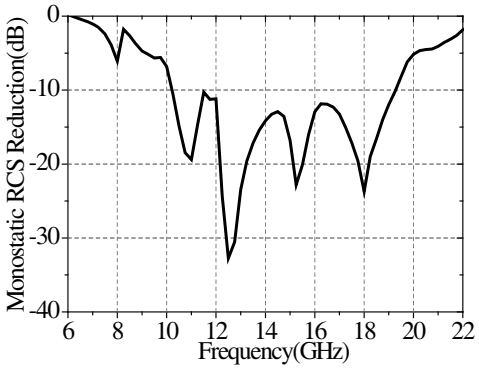

Figure 6. Simulated monostatic RCS reduction versus frequency under normal incidence.

2.3. Design of the Proposed PCM

According to the previous analysis, supposing that the x-polarized incident wave is completely converted into its orthogonal one after reflection, the reflected waves produced by the PCM unit cell and the mirror unit cell will be canceled out. Thus, we intend to reduce RCS by arranging the PCM unit cells and the mirror ones in a chessboard configuration.

To validate this hypothesis, a novel type of PCM is designed in a chessboard configuration, as shown in Fig. 5. The metasurface has an overall size of 70×70 mm and contains 14×14 unit cells. The PEC ground plane with equal-size is chosen as the reference one.

To study the scattering patterns and energy distribution of the PCM, the monostatic RCS reduction and scattered fields versus frequency for a normally incident wave are illustrated in Figs. 6 and 7, respectively. It can be observed from Fig. 6 that the 10 dB monostatic RCS reduction bandwidth of the PCM ranges from 10.2 to 19.3 GHz while the maximum reduction is 32.8 dB. Additionally, the results from above indicated that the monostatic RCS reduction band is consistent with the polarization conversion band shown in Fig. 2(a). The slight discrepancy is caused by the finite unit cells and edge effect. For an intuitive view, Fig. 7 presents the 3-D bistatic RCS patterns of the PEC ground and the PCM at 12.5 GHz. Under normal incidence, the RCS is significantly reduced near the normal direction with the appearance of four reflected lobes. That is to say, the RCS reduction near the normal direction is based on redirecting the energy in non-normal direction.

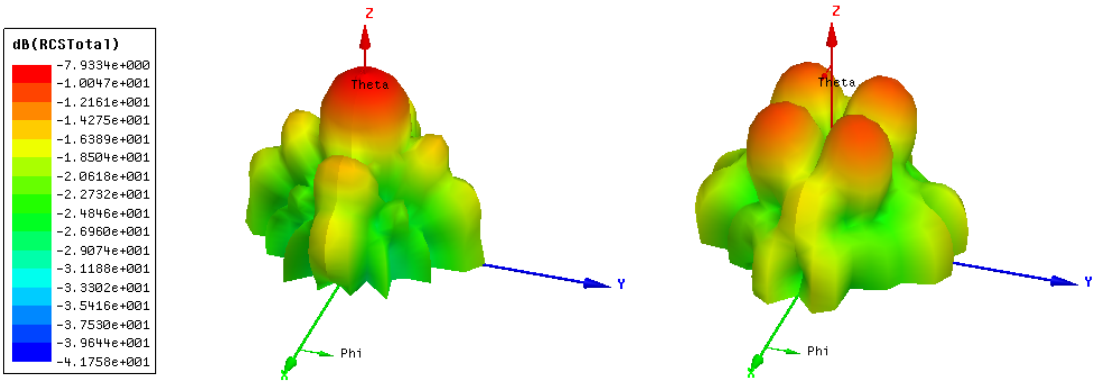

Figure 7. 3-D bistatic scattered fields at 12.5 GHz under normal incidence for (a) the PEC ground and (b) the PCM.

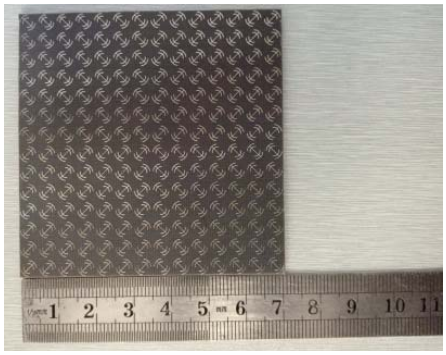

Figure 8. Photograph of the fabricated PCM.

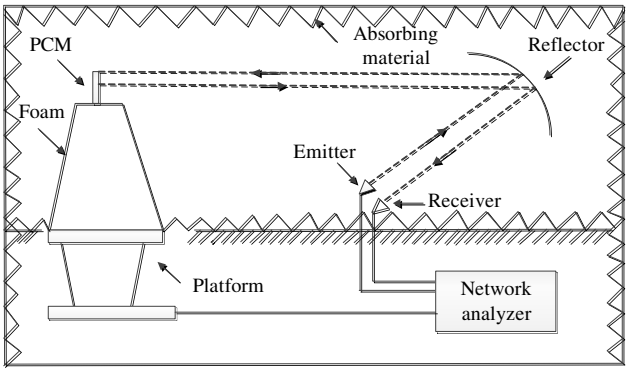

Figure 9. Schematic view of the RCS measurement setup in an anechoic chamber.

3. FABRICATION AND MEASUREMENTS OF PCM

To experimentally verify the design, the PCM is fabricated on a F4B-2 substrate and assembled. Fig. 8 presents a photo of the fabricated prototype. The schematic view of the experimental setup is shown in Fig. 9, in which three pairs of horn antennas are selected as emitters and receivers to cover the frequency band from 6–18 GHz. These correspond with the following bands: 5.8–8.2 GHz, 8.2–12.4 GHz and 12.4–18 GHz. Considering the limitations of experimental conditions, the measurement is conducted only in the range of 6–18 GHz. Simulations and measurements of the PCM are compared and analyzed in this section. The monostatic RCS patterns are discussed in detail, involving the effect of TE- and TM-polarization under oblique incidences.

3.1. Normal Incidence

The simulated and measured monostatic RCS results of the PCM versus frequency for normal incidence are depicted in Fig. 10. As expected, the measured RCS results match well with the simulated ones except some acceptable discrepancies which can be attributed to the following reasons: 1) the plane wave used in experiment is generated by the far-field radiation from the horn antennas while an ideal plane wave is used in simulation; 2) fabrication tolerance in the measurement setup.

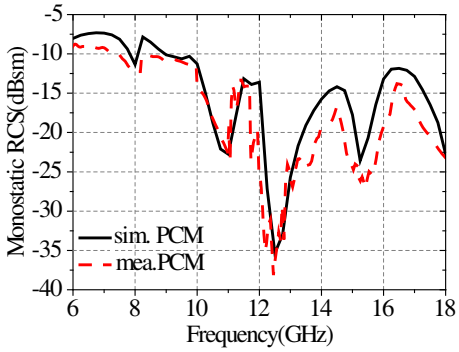

Figure 10. Simulated and measured monostatic RCS versus frequency under normal incidence.

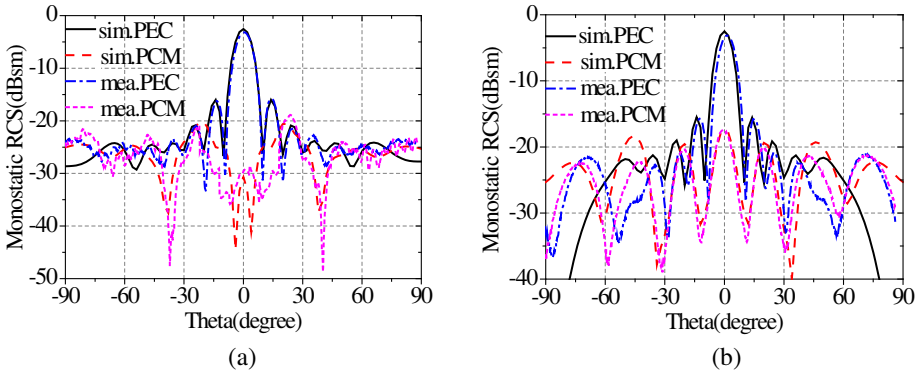

Figure 11. Simulated and measured monostatic RCS of PCM and PEC at 12.5 GHz versus the angles of incidence for (a) TE-polarization (the incident electric field parallel to the xoy plane, $\varphi = 90°$) and (b) TM-polarization (the incident magnetic field parallel to the xoy plane, $\varphi = 0°$).

3.2. Oblique Incidence

In view of the measurement results, the monostatic RCS of the PCM and the PEC ground plane with oblique incidence for TE- and TM-polarizations at 12.5 GHz are evaluated in Fig. 11. To better appreciate the comparison between measured and simulated results, the measured results are presented after a 3 deg misalignment correction. The 3deg misalignment is caused because the sample was placed not strictly perpendicular to the transmitting and receiving antennas. It can be seen that good agreement between simulations and measurements is obtained. Besides, RCS reduction is achieved when the angles of incident wave go within $\pm 18°$ for both polarizations. This phenomenon occurs because the PCR of RCS is highly dependent on the incident angles [10].

4. CONCLUSION

In this paper, a novel type of PCM for broadband RCS reduction is presented. The unit cell of the metasurface is composed of an oblique SRR and a cut-wire resonator, which shows the ability of converting a linear polarization state into its orthogonal one. The 10 dB bandwidth of polarization conversion is from 9.4 to 19.2 GHz, with an average PCR of nearly 100%. Due to the high PCR, a wide 10 dB monostatic RCS reduction bandwidth from 10.2 to 19.3 GHz is achieved with respect to the equal-sized PEC ground planes. For oblique incidences, the structure also works in a certain angle owing to the angular dependence of the PCR of RCS. To experimentally verify the proposed structure, prototypes of the PCM are fabricated and measured. The simulation results agree well with the measurement ones. The proposed metasurface has the advantages of simple geometry and broad band, which shows great potential applications in novel stealth technologies and materials.

ACKNOWLEDGMENT

This work was supported by the National Basic Research Program of China-973 program 2015CB857100, National Natural Science Foundation of China (No. 61401327, 61201018, 61471278), and Specialized Research Fund for the Doctoral Program of Higher Education of China (No. 20130203120011, 20120203120011).

REFERENCES

1. Thakare, Y. B. and Rajkumar, "Design of fractal patch antenna for size and radar cross-section reduction," *Microw. Antennas Propag.*, Vol. 4, No. 2, 175–181, Feb. 2010.
2. Pan, W. B., C. Huang, P. Chen, X. L. Ma C.-G. Hu, and X.-G. Luo, "A low-RCS and high-gain partially reflecting surface antenna," *IEEE Trans. on Antennas and Propag.*, Vol. 62, No. 2, 945–949, Feb. 2014.
3. Costa, F. and A. Monorchio, "A frequency selective radome with wideband absorbing properties," *IEEE Trans. on Antennas and Propag.*, Vol. 60, No. 6, 2740–2747, Jun. 2012.
4. Li, Y. Q., H. Zhang, Y. Q. Fu, and N. C. Yuan, "RCS reduction of ridged waveguide slot antenna array using EBG radar absorbing material," *IEEE Antennas and Wireless Propagation Letters*, Vol. 7, 473–476, 2008.
5. Paquay, M., J. C. Iriarte, I. Ederra, R. Gonzalo, and P. de Maagt, "Thin AMC structure for radar cross-section reduction," *IEEE Trans. on Antennas and Propag.*, Vol. 55, No. 12, 3630–3638, Dec. 2007.
6. De Cos, M. E., Y. Alvarez, and F. Las-Heras, "A novel approach for RCS reduction using a combination of artificial magnetic conductors," *Progress In Electromagnetics Research*, Vol. 107, 147–159, 2010.
7. Iriarte, J. C., A. T. Pereda, J. L. M. de Falcon, I. Ederra, R. Gonzalo, and P. de Maagt, "Broadband radar cross-section reduction using AMC technology," *IEEE Trans. on Antennas and Propag.*, Vol. 61, No. 12, 6136–6143, Dec. 2013.
8. Chen, W. G., C. A. Balanis, and C. R. Birtcher, "Checkerboard EBG surfaces for wideband radar cross section reduction," *IEEE Trans. on Antennas and Propag.*, Vol. 63, No. 6, 2636–2645, Jun. 2015.
9. Zheng, Y. J., J. Gao, X.-Y. Cao, Z.-D. Yuan, and H.-H. Yang, "Wideband RCS reduction of a microstrip antenna using artificial magnetic conductor structures," *IEEE Antennas and Wireless Propagation Letters*, Vol. 14, 1582–1585, 2015.
10. Liu, Y., K. Li, Y.-T. Jia, Y.-W. Hao, S. X. Gong, and Y. J. Guo, "Wideband RCS reduction of a slot array antenna using polarization conversion metasurface," *IEEE Trans. on Antennas and Propag.*, Vol. 64, No. 1, 326–331, Jan. 2016.
11. Jia, Y.-T., Y. Liu, Y. J. Guo, K. Li, and S. X. Gong, "Broadband polarization rotation reflective surfaces and their applications to RCS reduction," *IEEE Trans. on Antennas and Propag.*, Vol. 64, No. 1, 179–188, Jan. 2016.
12. Liu, Y., Y.-W. Hao, K. Li, and S. X. Gong, "Radar cross section reduction of a microstrip antenna based on polarization conversion metamaterial," *IEEE Antennas and Wireless Propagation Letters*, Vol. 15, 80–83, 2016.
13. Grady, N. K., J. E. Heyes, D. R. Chowdhury, Y. Zeng, M. T. Reiten, A. K. Azad, A. J. Taylor, D. A. R. Dalvit, and H.-T. Chen, "Terahertz metamaterials for linear polarization conversion and anomalous refraction," *Science*, Vol. 340, 1304–1307, Jun. 2013.
14. Gao, X., X. Han, W. P. Cao, H. O. Li, H. F. Ma, and T. J. Cui, "Ultrawideband and high-efficiency linear polarization converter based on double V-shaped metasurface," *IEEE Trans. on Antennas and Propag.*, Vol. 63, No. 8, 3522–3530, Aug. 2015.
15. Yu, N.-F., P. Genevet, M. A. Kats, F. Aieta, J. P. Tetienne, F. Capasso, and Z. Gaburro, "Light propagation with phase discontinuities: Generalized laws of reflection and refraction," *Science*, Vol. 334, 333–337, Oct. 2011.